34th Annual International Conference of the IEEE EMBS
San Diego, California USA, 28 August - 1 September, 2012

Investigation of the Electric Field Components of tDCS via Anisotropically Conductive Gyri-specific Finite Element Head Models

Mohamed K. Metwally, Young Sun Cho, Hae-Jeong Park, and Tae-Seong Kim, Member, IEEE

Abstract— **Transcranial Direct Current Stimulation (tDCS) is considered as one of the promising techniques for noninvasive brain stimulation and brain disease therapy. In this study, we have investigated the effect of skull and white matter (WM) anisotropy on the induced electric field (EF) by tDCS in two different montages; one using a pair of clinically used rectangular pad electrodes and the other 4(cathodes)+1(anode) ring electrodes. Using a gyri-specific finite element (FE) head model, we simulated tDCS and investigated the radial and tangential components of the induced EF in terms of their distribution over the cortical surface besides the distribution of the transverse and longitudinal components within WM. The results show that the tangential component of the EF on the cortical surface seems to be the main cause of the cortical stimulation of tDCS. Also WM anisotropy seems to increase the dispersion of the transverse component of the EF that affects the dispersion of the EF magnitude within the WM region.**

I. Introduction

Transcranial direct current stimulation (tDCS) is a promising technique for noninvasive brain stimulation. It modulates the membrane potentials of cortical neurons by injecting weak direct current (less than 2mA) into the brain using electrodes positioned on the scalp [1]. tDCS is suggested to relieve the symptoms of depression [2], stroke [3], [4], Parkinson's disease [5], and epilepsy [6]. Although tDCS is considered as a promising therapeutic technique, the induced electric field (EF) inside the brain is not well elucidated yet. Many types of head models have been utilized to simulate tDCS and studied the distribution of the current density (CD) and EF using finite element analysis (FEA). The initial trials involved using spherical head models [7], [8] which did not consider the complexity of the head geometry. Recently, MRI-derived high-resolution automatically realistic FE head models are used to investigate the influence of tissue anisotropy on the EF distribution [9], [10]. For instance, a gyri-specific head model was generated to compare the EF distribution due to two different montages and had studied the distribution of the EF and its components (radial and tangential components over the cortical surface). However, only isotropic conductivity was considered [11], [12] whereas the skull and white matter (WM) are known to be highly anisotropic [9].

Mohamed K. Metwally, Young Sun Cho, Tae-Seong Kim are with the Department of Biomedical Engineering, Kyung Hee University, Yongin, Gyeonggi, Republic of Korea (Tae-Seong Kim: +82-31-201-3731; fax: +82-31-201-3666; e-mail: tskim@khu.ac.kr).

Hae-Jeong Park is with the Department of Medical Science, College of Medicine, Yonsei University, Republic of Korea.

In this work, to have a better insight about the effect of tissue anisotropy (i.e., the skull and WM) on the distribution of the EF and its components, we have done simulation studies via 3-D MRI-derived high-resolution gyri-specific FE head models, incorporating tissue anisotropic properties in the skull and WM. Two different montages have been investigated: one using the conventional clinically used pad electrodes, the other using the 4+1 ring electrodes. The results show the strong influence of the tissue anisotropy on tDCS and the tangential and the transverse components of the induced EF as a major stimulation causes.

II. Method

A. Generations of 3-D Gyri Specific FE Head Models

Our model was generated from 146 MR images acquired on a 3-T MRI scanner. Each slice has dimensions of 212 x 181 with a voxel volume of 1 mm^3. The head model was segmented into five tissues: WM, gray matter (GM), cerebrospinal fluid (CSF), skull, and scalp. Segmentation and meshing were done using Freesurfer [13], in-house morphological technique [14], and ISO2MESH [15].

B. tDCS Montages

Two montages were used; (1) rectangular pad electrode; and (2) 4(cathodes) +1(anode) ring electrodes. Fig. 1 shows the rendered 3-D head for each montage. The rectangular pad electrodes were simulated with a size of 5 cm × 7 cm for each electrode. The anode was centered at C3 based on the international 10-20 EEG system, while the cathode was over the right eyebrow to stimulate the motor cortex. On the other hand, the ring configuration montage was simulated using a set of cylindrical electrodes. Each electrode has a radius of 4 mm and height of 2 mm. The anode was placed over C3 and the cathodes were positioned over the corners of the rectangular pad.

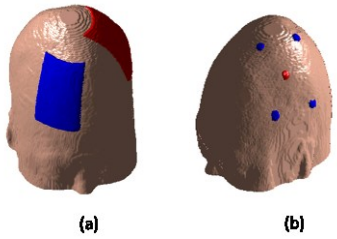

Fig. 1 3-D rendered tDCS montages (a) rectangular pad montage with anode (in red) at C3 and cathode (in blue), and (b) ring electrodes with anode (in red) over C3 and cathodes (in blue) over corners of the rectangular pad electrode.

C. *Isotropic and Anisotropic Conductivity Setup*

Two types of conductivity settings have been used for both montages. The first one was isotropic in both of the skull and WM, while the second one considering the skull and WM anisotropy. The following isotropic conductivity values were set in the isotropic head models: WM=0.14 S/m, GM=0.33 S/m, CSF=1.79 S/m, skull=0.0132 S/m, and scalp= 0.33 S/m [16]. For the anisotropic model, we assumed the electric conductivity within WM parallel to the direction of the neural fibers (i.e., longitudinal direction) is 10 times larger than that in the normal direction (i.e., transverse direction). The same ratio was adopted for the skull anisotropic conductivity where the conductivity in the tangential direction to the surface is 10 times larger than that in the perpendicular direction (i.e., radial direction) [17]. Using the eigen vectors from DT-MRI (based on an assumption that the diffusion and conductivity tensors share the same eigen vectors, and according to the volume constraint algorithm [17]), we assigned the conductivity values for the skull to be 0.002844 S/m and 0.02844 S/m in the radial and tangential directions respectively while for WM the values were 0.65 S/m and 0.065 S/m in the longitudinal and transverse directions respectively.

D. *tDCS Simulation*

A current amount of 1mA was injected into the anode and extracted from the cathode in the case of the rectangular pad montage, while in the case of ring montage, a current amount of 2mA was injected by the anode and 0.5 mA was extracted by each cathode. The conductivity of the electrodes was assigned as 5.8×10^7 S/m. The EF distribution in the head was computed by solving the following quasi-static Laplace equation:

$$\nabla.(\sigma\nabla V)= 0 \qquad (1)$$

where V is electric potential and σ is the electrical conductivity of the tissue. The sparse direct equation solver in ANSYS based on the direct elimination of equation was used to calculate the induced EF in the whole head [18].

III. RESULTS

The radial direction within GM was defined to be in the normal direction to the gyri or sulci surface pointing towards the CSF, and the longitudinal direction within WM was defined to be parallel to the neuron fiber direction. The tangential and transverse component was defined to be the second norm of the EF components in the perpendicular plane to the radial direction and the longitudinal direction respectively.

TABLE I. Quantitative results from rectangular pad montage of the cortical surface and GM

Model	Feature	Surface Area (mm^2)	GM Volume (mm^3)	Maximum EF (V/m)
Isotropic	***Magnitude***	25983	70414	0.23
	Radial	2210	10409	0.18
	Tangential	18359	46819	0.23
Anisotropic	***Magnitude***	13459	37470	0.16
	Radial	1210	4697	0.15
	Tangential	8694	22508	0.14

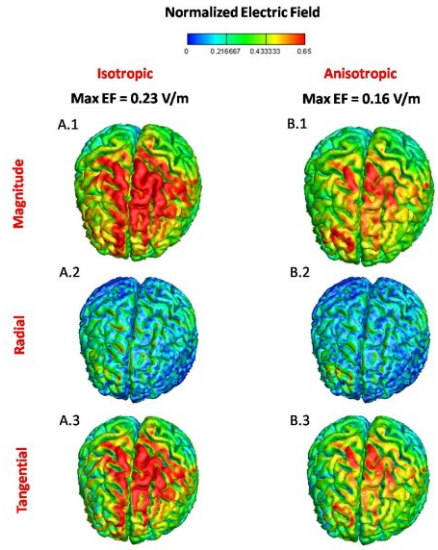

Fig. 2 Column **A** shows the results from the isotropic model. Column **B** shows the results from the anisotropic model in the case of the rectangular pad montage. The first row shows the distribution of EF magnitude, the second, the distribution of the radial component, and the third, the distribution of norm of tangential component over the cortical surface.

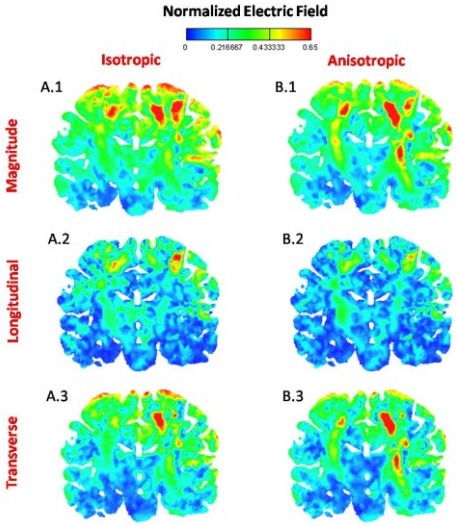

Fig. 3 Column **A** shows the results from the isotropic model. Column **B** shows the results from the anisotropic model in case of the rectangular pad montage. The first row shows the distribution of EF magnitude, the second, the distribution of the longitudinal component, and the third, the distribution of norm of transverse component within a coronal slice.

TABLE II. Quantitative results from the rectangular pad montage of WM

Model	Feature	WM Volume (mm^3)
Isotropic	***Magnitude***	92470
	Longitudinal	20221
	Transverse	47405
Anisotropic	***Magnitude***	82078
	Longitudinal	11294
	Transverse	57272

The affected region (either area or volume) was defined to be the region that encompasses elements that have EF larger than the half-maximum of the induced EF magnitude [20].

A. Rectangular Pad Montage

Fig. 2 shows the distribution of magnitude, radial, and the norm of tangential components of EF over the cortical surface. Fig. 3 shows the distribution of magnitude, longitudinal, and the norm of the transverse components of EF within a coronal slice under the anode. A.1, A.2, and A.3 in Figs. 2 and 3 are from the isotropic model, while B.1, B.2, and B.3 from the anisotropic model. Note that the EF was normalized in each figure. Tables I and II show the quantitative results for the rectangular pad montage. The quantitative measurements include the maximum EF, which is on the cortical surface, in magnitude, radial, and the norm of tangential components within each model (i.e., isotropic and anisotropic) in addition to the area and volume of the affected regions.

High EF was observed under the rim of the electrodes especially at the corners, besides observing high EF on the walls and deep bottoms of sulci. The sulci area that is affected by the high EF is expanded after considering the tissue anisotropy (not shown here). In addition, the distribution of the norm of tangential component is almost same as that of the magnitude of EF on the cortical surface as shown in A.3 and B.3 in Fig. 2. Quantitatively, the tangential component covers in average about 68% of the affected area by the EF magnitude in the case of the rectangular pad montage.

The skull shunting in the anisotropic model is in effect by reducing the affected cortical surface area about 48% and dropping the maximum induced EF about 30%.

As shown in A.1 and B.1 in Fig. 3, the effect of the WM anisotropy on the distribution of EF was observed where EF becomes more diffused within WM. This great dispersion within WM might be resulted from the effect of the WM anisotropy on the transverse component of the induced EF as shown in A.3 and B.3 in Fig. 3. Table II shows that the affected WM volume by the transverse component in the anisotropic model increased about 21% more than that of the isotropic case.

B. Ring Montage

Fig. 4 shows the distribution of magnitude, radial, and the norm of tangential components of EF over the cortical surface. Fig. 5 shows the distribution of magnitude, longitudinal, and the norm of transverse components of EF within a coronal slice under the anode. A.1, A.2, and A.3 in

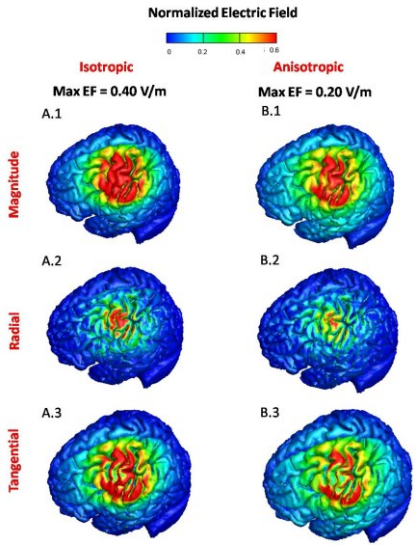

Fig. 4 Column **A** shows the results from the isotropic model. Column **B** shows the results from the anisotropic model in case of ring configuration montage. The first row shows the distribution of EF magnitude, the second, the distribution of the radial component, and the third, the distribution of norm of the tangential component over the cortical surface.

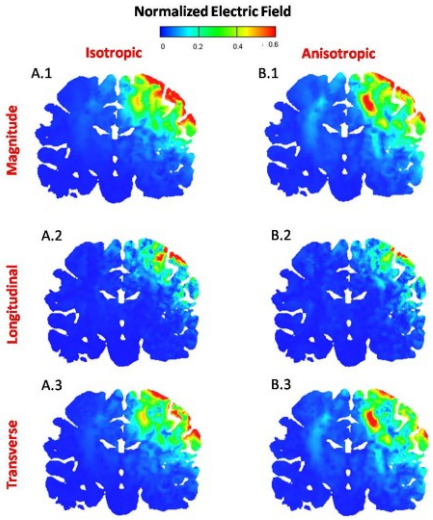

Fig. 5 Column **A** shows the results from the isotropic model. Column **B** shows the results from the anisotropic model in case of ring configuration montage. The first row shows the distribution of EF magnitude, the second, the distribution of the longitudinal component, and the third, the distribution of norm of transverse component within a coronal slice.

TABLE III. Quantitative results from the ring montage of the cortical surface and GM

Model	Feature	Surface Area (mm^2)	GM Volume (mm^3)	Maximum EF (V/m)
Isotropic	***Magnitude***	6354	13247	0.4
	Radial	848	2287	0.34
	Tangential	5223	10268	0.39
Anisotropic	***Magnitude***	4023	8177	0.2
	Radial	489	1034	0.17
	Tangential	2844	5412	0.19

TABLE IV. Quantitative results from the ring montage of WM

Model	Feature	WM Volume (mm^3)
Isotropic	***Magnitude***	5718
	Longitudinal	1034
	Transverse	3774
Anisotropic	***Magnitude***	11700
	Longitudinal	345
	Transverse	9594

Figs. 4 and 5 are from the isotropic model, while B.1, B.2, and B.3 from the anisotropic model. Tables III and IV show the quantitative results for the ring montage. High EF was observed on the wall of sulci (not shown here).

Skull anisotropy seems to have an effect to reduce the maximum induced EF over the cortical surface about 50% less than that in the case of the isotropic model. As shown in A.1 and B.1 in Fig. 4, the EF distribution over the cortical surface was reduced in the anisotropic model about 37% as reported in Table III which we believe due to the shunting effect of the skull anisotropy.

A.1 and B.1 in Fig. 5 show the effect of WM anisotropy to modulate regions within WM where the affected volume of WM was increased 2 times more than that within WM in the isotropic case. From A.3 and B.3 in Fig. 5, we can see that this effect is mainly due to the contribution of the transverse component of the induced EF. In average, the tangential component of the EF covers about 76% of the cortical surface area that is covered by the EF magnitude.

IV. DISCUSSION

This study has investigated the distribution of the induced EF and its components in two different montages and the effect of the tissue anisotropy on these distributions. The skull anisotropy enhances the focality of the radial component obviously in the case of the ring montage more than the rectangular pad. Although the maximum induced EF in the isotropic case with the ring montage is almost double that in the case of the rectangular pad, the skull anisotropy has affected the maximum induced EF in both montages to be closer to each other. The WM anisotropy seems to increase the dispersion of EF within WM more obviously in the case of the rectangular montage than the ring. This study shows greater contribution of the tangential and the transverse components to the EF distribution on the cortical surface and within the WM respectively.

V. CONCLUSION

This study aims to have a better insight about the components of the induced EF (i.e., radial and tangential on the cortical surface, and longitudinal and transverse within WM) and the influence of tissue anisotropy on their distributions. The study shows that the tangential component has a great contribution on the EF distribution on the cortical surface and covers most of the affected regions by the EF magnitude. Also the WM anisotropy increases the dispersion of the transverse component within the WM region which results in increasing the EF dispersion within the WM region.

ACKNOWLEDGMENT

This work was supported by the National Research Foundation of Korea (NRF) grant funded by the Korea government (MEST) (2011-0029485) and (2010-0020676).

REFERENCES

[1] M. A. Nitsche, and W. Paulus,"Excitability changes induced in the human motor cortex by transcranial direct current stimulation," J. physiol., vol. 527.3, pp. 633-639, 2000.

[2] M. A. Nitsche, S. B. Paulus, F. Fregni, and P. Leone,"A Treatment of depression with transcranial direct current stimulation (tDCS): A Review," Exp. Neurology., vol. 219, pp. 14-19, 2009.

[3] F. C. Hummel, and L. G. Cohen,"Non-invasive brain simulation: a new strategy to improve neurorehabilitation after stroke?," Lancet Neurol., vol. 5, pp.708-712, 2006.

[4] T. Wagner, F. Fregni, S. Fecteat, A. Grodzinsky, and M. Zahn, "Transcranial direct current stimulation: a computer-based human model study," NeuroImage, vol. 35, pp. 1113-24, 2007.

[5] F. Fregin, P. S. Boggio, M. C. Santos, M. Lima, A. L. Vieira, S. P. Rigonatti, M. T. Silva, E. R. Barbosa, M. A. Nitsche, and A. Pascual-Leone,"Noninvasive cortical stimulation with transcranial direct current stimulation in Parkinson's disease," Movement Disorders, vol. 21, pp. 1693-1702, 2006.

[6] F. Fregin, S. Thome-Souza, M. A. Nitsche, S. D. Freedman, K. D. Valente, and A. Pascual-Leone,"A controlled clinical trial of cathodal DC polarization in patients with refractory epilepsy," Epilepsia, vol. 75, pp. 335-342, 2006.

[7] A. Datta, M. Elwassif, F. Battaglia, M. Bikson," Transcranial current stimulation focality using disc and ring electrode configurations: FEM analysis". J. Neural Eng. 5,pp. 163–174. 2008

[8] P. C. Mirandaa, M. Lomarevb, and M. Hallettb, "Modeling the current distribution during transcranial direct current stimulation". Clinical Neurophysiology, Volume 117, pp. 1623-1629, 2006.

[9] H. S. Suh, S. H. Kim, W. H. Lee, T. S. Kim," Realistic Simulation of Transcranial Direct Current Stimulation via 3-D High-resolution Finite Element Analysis: Effect of Tissue Anisotropy". EMBC 2009. Annual International Conference of the IEEE, pp. 638 – 641,2009.

[10] H. S. Suh, W. H. Lee, Y. S. Cho, J. H. Kim, and T. S. Kim, "Reduced Spatial Focality of Electrical Field in tDCS with Ring Electrodes Due to Tissue Anisotropy". EMBC 2010. Annual International Conference of the IEEE, pp. 2053 - 2056,2010.

[11] A. Datta, V. Bansal, J. Diaz, J. Patel, D. Reato, M. Bikson, "Gyri-precise head model of transcranial direct current stimulation: improved spatial focality using a ring electrode versus conventional rectangular pad". Brain Stimul. pp. 201–207, 2009.

[12] R. Salvador, A. Mekonnen, G. Ruffini, P. C. Miranda. "Modeling the electric field induced in a high resolution realistic head model during transcranial current stimulation". IEEE EMBS 2010.

[13] http://surfer.nmr.mgh.harvard.edu/

[14] B. Dogdas, D. W. Shattuck, R. M. Leahy, "Segmentation of skull and scalp in 3-D human MRI using mathematical morphology". Hum Brain Mapp. pp. 273-85, 2005.

[15] ISO2MESH Available: http://iso2mesh.sourceforge.net

[16] S. Kim, T. S. Kim, Y. Zhou, and M. Singh, "Influence of conductivity tensors on the scalp electrical potential: Study with 2-D finite element models," IEEE Trans. Nucl. Sci., vol. 50, pp. 133-138, 2003.

[17] C. H. Wolters, A. Anwander, X. Tricoche, D. Weinstein, M. A. Koch, and R. S. Macleod, "Influence of tissue conductivity anisotropy on EEG/MEG field and return current computation in a realistic head model: A simulation and visualization study using high-resolution finite element modeling," NeuroImage, vol. 30, pp. 813-826, 2006.

[18] ANSYS. Available: http://www.ansys.com/

[19] M. Sekino and S. Ueno, "Comparison of current distributions in electroconvulsive therapy and transcranial magnetic stimulation," J. Appl. Phys., vol. 91, no.10, pp. 8730-8732, 2002

[20] Z. D. Deng, S. H. Lisanby, A. V. Peterchev, "Electric field strength and focality in electroconvulsive therapy and magnetic seizure therapy: a finite element simulation study". Journal of neural engineering, vol. 8, 13 pp. 2011.